

Slot jet impingement heat transfer for the cases of moving plate and moving nozzle

Mostafa Rahimi¹ · Roghayeh Azimi Soran¹

Received: 23 July 2015 / Accepted: 28 January 2016 / Published online: 12 February 2016
© The Brazilian Society of Mechanical Sciences and Engineering 2016

Abstract Jet impingement heat transfer for the case of extended surfaces is usually accomplished by employing arrays of impinging jets. Both the cases of moving plate and moving nozzle could be other options to transfer heat to/from the extended surfaces, which has been investigated numerically at the present study. Heat transfer distribution on a hot stationary flat plate was first specified for an unconfined slot laminar air jet impinging on the plate. Air jet Reynolds number and nozzle-to-plate separation were $Re = 500$ and $H/W = 5$, respectively. The effects of the moving plate and moving nozzle were then separately examined on both the flow and thermal fields. The distribution of the local Nusselt numbers was presented for a range of moving nozzle and moving plate. The analysis revealed that the Nusselt number decreased as the velocity of the plate or the nozzle was increased, where the effect of the moving nozzle was relatively substantial.

Keywords Impingement heat transfer · Moving plate · Moving nozzle · Nusselt number

List of symbols

c_p Specific heat of air at constant pressure (1006.43 J/kg-K)
 H Nozzle-to-plate separation (m)
 h Convective heat transfer coefficient (W/m^2-K)
 k Thermal conductivity of air (0.0242 W/m-K)
 Nu Nusselt number (hW/k)

p Pressure (N/m^2)
 Re Jet Reynolds number ($\rho V_j W/\mu$)
 T Temperature (K)
 t Time (sec)
 u x -Velocity component (m/s)
 V Velocity (m/s)
 v y -Velocity component (m/s)
 W Width of the slot nozzle (m)
 X Dimensionless longitudinal direction (x/W)
 x Cartesian coordinate (m)
 y Dimensionless normal direction (y/W)
 Y Cartesian coordinate (m)
 y_1 Distance of the first grid line from the solid surface (mm)
 y_2 Uniform grid size far from the solid surface (mm)

Greek symbols

ρ Air density (1.225 kg/m^3)
 μ Air dynamic viscosity (1.7894×10^{-5} kg/m-s)

Subscripts

j Jet
 n Nozzle
 p Impinged plate

1 Introduction

There have been many studies of heat transfer to/from an air jet that is impinging onto a surface which is perpendicular to the jet axis. The incentive for the studies is often related to heating and cooling, or drying processes, and the majority is confined to the cases in which both the plate and the nozzle are stationary. Considering the number of practical applications such as thermal processing of

Technical Editor: Jose A. dos Reis Parise.

✉ Mostafa Rahimi
rahimi@uma.ac.ir

¹ Department of Mechanical Engineering, University of Mohaghegh Ardabili, P.O. Box 179, Ardabil, Iran

extended metal and glass sheets and drying of paper and textiles, where air jets impinge upon a moving flat surface and heat transfer is involved, surprisingly little published data are available. Moreover, for the case of moving nozzle no more study is found in the published literature.

Some of the earliest measurements of heat transfer from a continuously moving belt to an impinging slot jet were made by Raju and Schlünder [5]. An infrared thermometer was used for the measurement of temperature of the moving belt and heat transfer was assumed to be affected by the jet velocity ($4 < V_n < 40$ m/s), the jet width ($4.8 < W < 19$ mm), the nozzle-to-plate distance ($3 < H/2W < 11$) and the belt speed ($0.15 < V_p < 5.5$ m/s). The results showed that the average heat transfer coefficient increased with belt speed steeply initially to a maximum value and then remained almost constant for all the higher belt speeds. The maximum heat transfer coefficient was about 1.5–2.0 times higher than that predicted for the stationary surface. Zumbunnen, Incropera and Viskanta [9] developed a theoretical model of planar jet impingement heat transfer on a moving plate. Boundary layer equations in their integral forms were used to include the effects of surface motion directed perpendicular to the jet plane, an arbitrary surface temperature variation and non-uniform jet discharge velocity profiles. Results indicated that the influence of non-uniform jet discharge velocity decreased with distance from the stagnation line. Surface motion affected heat transfer at regions away from the stagnation line, but has little influence near the stagnation line when the surface temperature was constant. Yang and Hao [8] numerically predicted the flow field and heat transfer characteristics for three turbulent impinging slot jets. The interesting parameters included in the study were: entrance Reynolds number (Re), dimensionless nozzle-to-surface space (H/W), dimensionless pitch (P/W) and dimensionless velocity ratio (V_p/V_j). The computed results showed that the dimensionless pitch had a strong influence on the heat transfer characteristics. In the case with surface motion, it was found that the skin friction coefficient of the impinging surface was strongly affected by the surface motion, but the heat transfer characteristic was not significant in the range of $0.05 \leq V_p/V_j \leq 0.25$. Chattopadhyay et al. [1] conducted a numerical study to investigate turbulent flow field and heat transfer in an array of slot jets impinging on a moving surface. The surface velocity, directed perpendicular to the jet, was varied up to two times of the jet velocity measured at the nozzle exit. It was found that an increase of the velocity of the impingement plate reduces heat transfer, on the other hand distribution of Nusselt number became more uniform with the increased surface velocity. In a similar study, Chattopadhyay and Saha [2] examined the laminar flow and heat transfer on a moving surface due to a bank of impinging slot jets and similar results for heat transfer distribution were obtained.

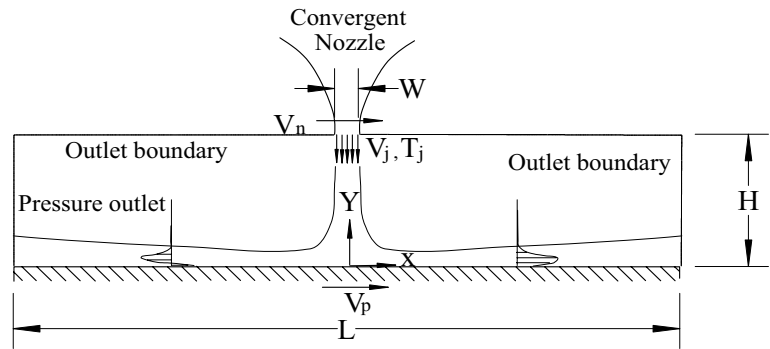
Senter and Sollicec [6] experimentally investigated the flow field of a confined turbulent slot air jet impinging normally on a moving flat surface. Experiments were conducted for a nozzle-to-plate spacing of eight slot nozzle widths, at three jet Reynolds numbers ($Re = 5300, 8000,$ and $10,600$) and four surface-to-jet velocity ratios of 0, 0.25, 0.5, and 1. It appeared that the flow field patterns at a given surface-to-jet velocity ratio are independent of the jet Reynolds number in the range of 5300–10,600. A slight modification of the flow field was observed for a surface-to-jet velocity ratio of 0.25 whereas at higher ratios of 0.5 and 1, the flow field was significantly affected. Sharif and Banerjee [7] studied convective heat transfer from a moving isothermal hot plate to a confined slot impinging jet. The rectangular flow geometry consisted of a confining adiabatic wall placed parallel to the moving impingement surface with the slot jet located in the middle of the confining wall. The $k-\epsilon$ turbulence model with enhanced wall treatment was used for the turbulence computations. The problem parameters were the jet exit Reynolds number, ranging from 5000 to 20,000, the normalized plate velocity, ranging from 0 to 2, and the normalized distance of separation between the impingement plate and the jet exit, ranging from 6 to 8. The analysis revealed that the average Nusselt number increased considerably with the jet exit Reynolds number as well as with the plate velocity. The average skin friction coefficient, on the other hand, was relatively insensitive to the jet Reynolds number but increased significantly with the plate velocity.

It is seen from the published literature that the study of heat transfer from a moving plate due to an unconfined slot jet impingement has not been conducted yet and no report is found for the case of moving nozzle. To investigate convective heat transfer from a hot plain surface to an impinging slot air jet for the cases of moving nozzle and moving plate, present study has been conducted. Because of similar trends in heat transfer distribution obtained for different jet Reynolds numbers and nozzle-to-surface separations, a constant jet Reynolds number, $Re = 500$, and one dimensionless nozzle-to-surface separation, $H/W = 5$ were examined. Dimensionless velocity ratio for both the plate and the nozzle ranged from 0.1 up to a value for which the enhanced heat transfer no longer persisted on the stagnation region. The details of the flow field and heat transfer distribution were obtained for each case using numerical analysis.

2 Mathematical formulation

The geometry and coordinate system of the flow domain are shown in Fig. 1. It consists of a hot moving flat surface having length L at the bottom, on which one slot nozzle of

Fig. 1 Geometry and coordinate system of the computational domain



width W is located by a distance of H where the exit plane of the nozzle is parallel to the impingement plate. Both the plate and the nozzle are considered to move towards the right in turn, with a prescribed normalized velocity using the nozzle exit uniform velocity as the reference velocity. The working medium is assumed to be air with constant physical properties and the flow is considered to be two dimensional, laminar and incompressible. Cartesian coordinate system as indicated in Fig. 1 is used in the numerical analysis. Transient form of the conservation equations of the mass, momentum and energy for the flow under these circumstances are written as.

$$\frac{\partial u}{\partial x} + \frac{\partial v}{\partial y} = 0 \tag{1}$$

$$\frac{\partial u}{\partial t} + u \frac{\partial u}{\partial x} + v \frac{\partial u}{\partial y} = -\frac{1}{\rho} \frac{\partial P}{\partial x} + \frac{\mu}{\rho} \left(\frac{\partial^2 u}{\partial x^2} + \frac{\partial^2 u}{\partial y^2} \right) \tag{2}$$

$$\frac{\partial v}{\partial t} + u \frac{\partial v}{\partial x} + v \frac{\partial v}{\partial y} = -\frac{1}{\rho} \frac{\partial P}{\partial y} + \frac{\mu}{\rho} \left(\frac{\partial^2 v}{\partial x^2} + \frac{\partial^2 v}{\partial y^2} \right) \tag{3}$$

$$\frac{\partial T}{\partial t} + u \frac{\partial T}{\partial x} + v \frac{\partial T}{\partial y} = \frac{k}{\rho c_p} \left(\frac{\partial^2 T}{\partial x^2} + \frac{\partial^2 T}{\partial y^2} \right) \tag{4}$$

As indicated in Fig. 1, three types of boundary conditions including the inlet boundary, stationary or moving wall boundary and the outlet boundary were considered at the borders of the computational domain. Air jet flow with uniform velocity and constant temperature was assumed to enter into the domain from the inlet section which was the nozzle exit plane. No-slip wall boundary condition with a prescribed uniform wall heat flux was defined for the wall section and finally, zero gradients were assumed for all the quantities at the right outlet boundaries. For the case of moving plate, some shear-driven backflow through the left boundary into the domain is expected whereas, it is quantitatively unknown. Therefore, constant pressure outlet was defined on the left exit plane as the flow boundary

condition. By this definition, the exit plane pressure is taken as the average of the adjacent inside node pressure and the ambient constant pressure and the velocity components are extrapolated from the inside domain. The temperature of the backflow condition was taken as the nozzle exit condition.

3 Numerical procedure

Implicit pressure-based finite volume approach was employed in the present numerical analysis. The convective terms were discretized using the second-order upwind scheme while central difference scheme was used for the diffusion terms. A second-order Euler method was also used for time discretization in the case of transient analysis. The velocity and pressure terms in the momentum equations were coupled by the well-known SIMPLE algorithm. The equations were then solved using an iterative procedure to obtain the variables. The solution was considered to be converged when the normalized residuals were less than 10^{-6} in the energy equation and less than 10^{-3} in the other equations. The numerical analysis was conducted using Fluent 6.3 commercial software.

To obtain an appropriate grid distribution, a systematic grid resolution test was first conducted. For this purpose, three uniform grids were generated within the computational domain having 2, 1 and 0.5 mm dimensions. Then, the number of the horizontal grid lines was increased to produce more dense grids at the vicinity of the impinged plate. The distance between the plate and the first grid line ranged from 0.01 mm to 1 mm and a growth factor of 1.2 was applied in the vertical direction to reach the uniform grid size being constant in the rest of the domain. Using the generated grids, the numerical analysis was conducted for the case of a stationary plate with jet Reynolds number of 500 and $H/W = 5$. The distributions of the local Nusselt number on the stationary impinged plate are shown in Fig. 2 for several test cases. This figure indicates that a very approximate result is obtained using uniform coarse grid with 2 mm dimension. However, the accuracy of the

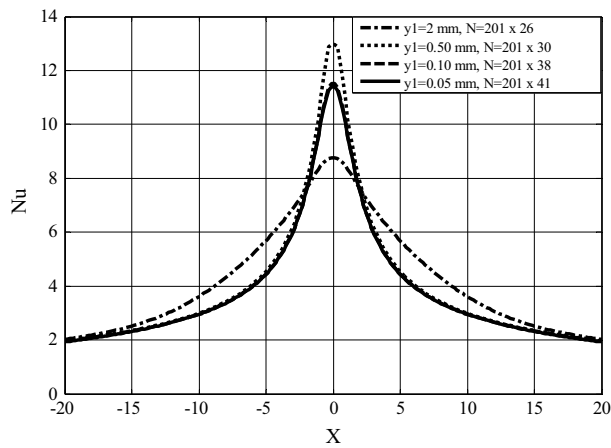
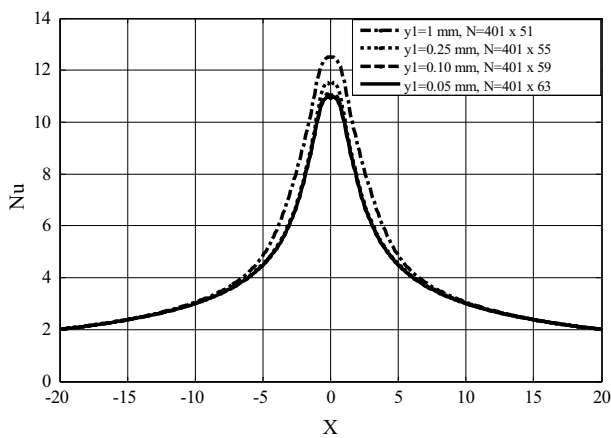
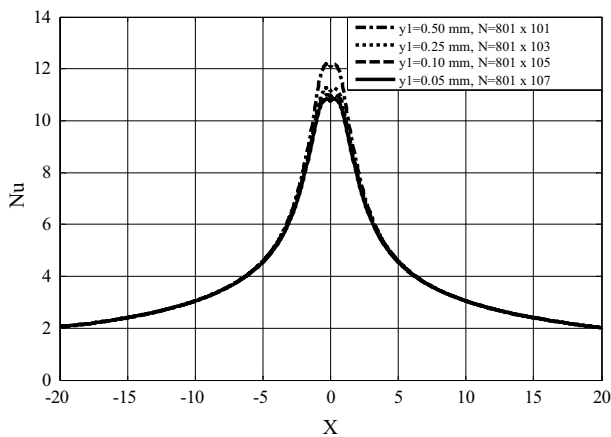
(a) $y_2 = 2$ mm(b) $y_2 = 1$ mm(c) $y_2 = 0.50$ mm

Fig. 2 Nusselt number distribution for grid independence analysis, $Re = 500$, $H/W = 5$

results are improved by clustering the grids close to the impinging surface (Fig. 2, case a). Convincing results are achieved using uniform grids with 1 mm dimension and the results are again converged to a certain distribution

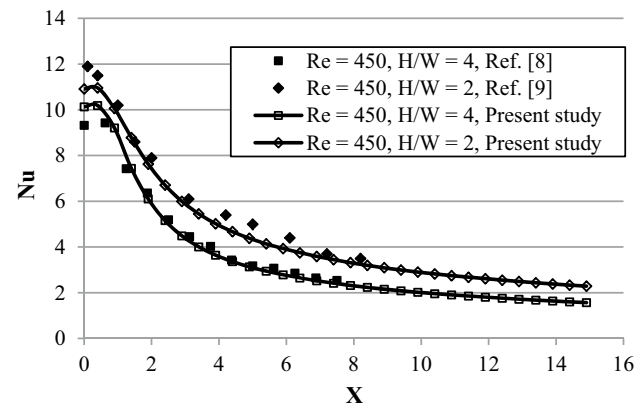


Fig. 3 Comparison of the local Nusselt number over the stationary flat plate

decreasing the grid size close to the solid surface (case b). Finally, quite similar results with the previous case are obtained using very dense grids within the computational domain (case c). Considering the results of the three examined cases, the distance between the first grid line and the plate was selected to be 0.1 mm. This size was increased by the same growth factor of 1.2 getting far from the plate to reach 1 mm and this value was kept constant at the rest of the domain. In this way, the total number of 401×59 grid points was employed within the computational domain having 5 cm height and 40 cm length.

The length of the plate was then altered to verify the effect of the imposed boundary conditions on the numerical results. Nusselt number distributions were then obtained for the same grids and under the same physical circumstances for the two cases of $-0.25 < x/W < 0.25$ and $-0.15 < x/W < 0.15$. The results indicated that the Nusselt number distribution on the impinged plate is not affected by the plate length in the examined range of this parameter. To prove correct prediction of the Nusselt number distribution on the impingement plate, a comparison was also made between present, Rady and Arquís's [4] and Miyazaki and Silberman's [3] studies. Figure 3 presents the results for laminar impinging air jet over stationary flat plate and under the same circumstances. It is seen that the predictions agree reasonably well with these experimental results.

To investigate the effect of the moving plate on the flow and thermal fields, no-slip boundary condition was employed in the steady numerical analysis. For the case of moving nozzle, transient form of the conservation equations was employed using the same geometry and coordinates. The time interval in the numerical analysis was calculated from;

$$\Delta t = 0.001/V_n \quad (5)$$

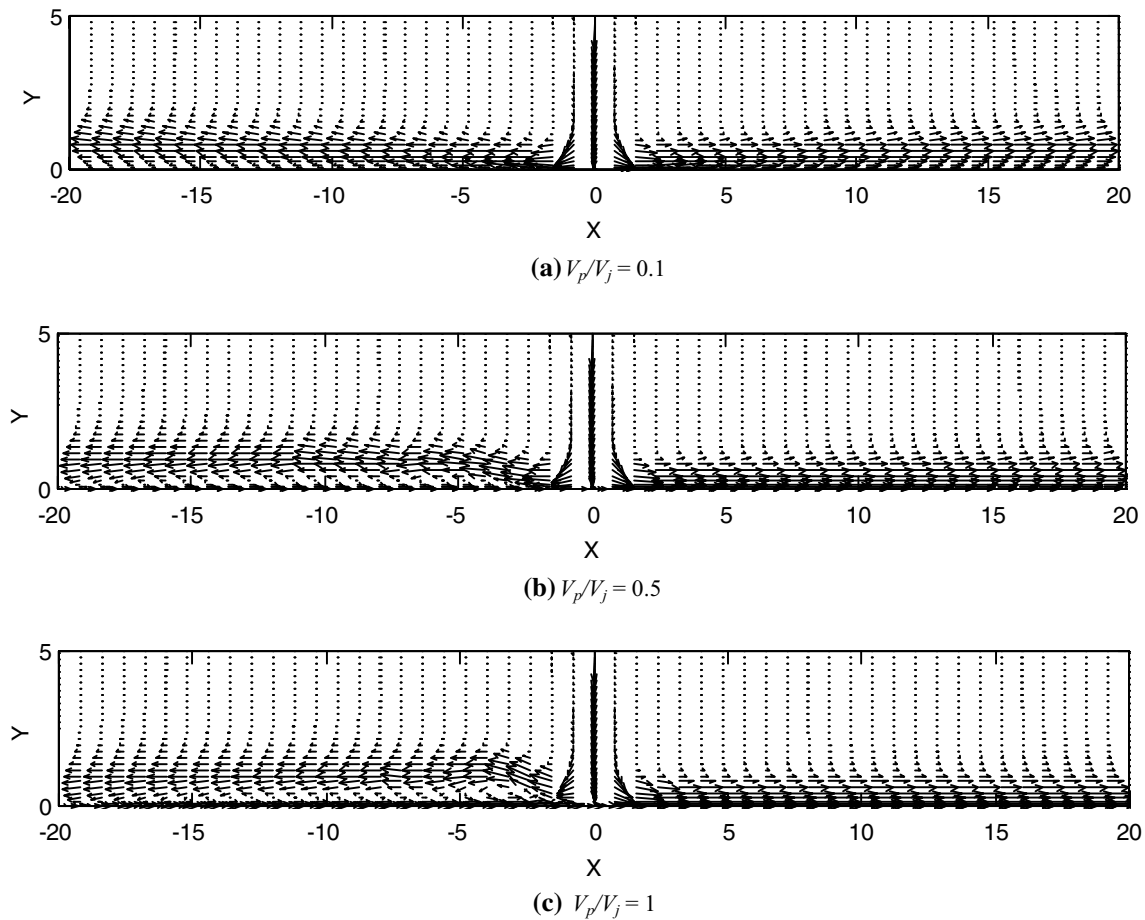


Fig. 4 Velocity vectors for the case of moving plate, $Re = 500$, $H/W = 5$

where V_n was the nozzle traveling velocity and 0.001 m was the mesh size at the nozzle exit plane. The converged flow and thermal fields were first determined at the end of the prescribed time interval, Δt , using the initial stationary conditions. Then, the position of the inlet boundary was shifted one grid on the upper horizontal boundary resembling the displacement of the nozzle. Transient forms of the conservation equations were then sequentially utilized to calculate the velocity, pressure and the temperature distributions while the converged values of these parameters at the end of each time step were used as the initial conditions in the next iteration. The numerical analysis was repeated for different values of the time interval and each turn the flow and thermal field parameters were specified.

4 Results and discussion

The analysis was first performed for the case of moving plate. The steady form of the conservation equations was considered and the moving solid boundary condition was applied in the numerical analysis. Figure 4 illustrates the

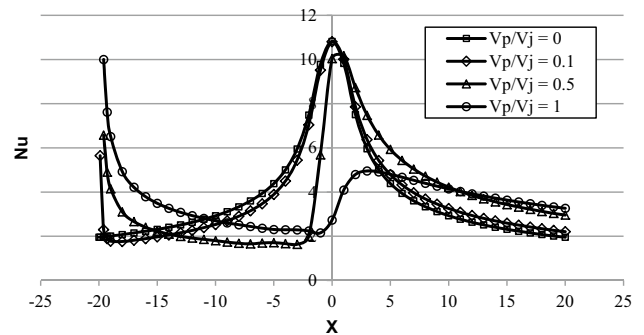


Fig. 5 Nusselt number distribution on the moving plate, $Re = 500$, $H/W = 5$

velocity vectors at $Re = 500$ and $H/W = 5$ for a moving plate with normalized velocity of $V_p/V_j = 0.1, 0.5,$ and 1 as representative cases. For the sake of higher clarity, the velocity vectors are shown in a quite fewer grid points at these plots. Consistent with these flow fields, the Nusselt number distributions are shown in Fig. 5. Moreover, the Nusselt number distribution over the stationary plate is also

presented in this figure. For the stationary plate case, the jet splits into two symmetrical wall jets as the jet impinges on the flat plate and, therefore, a symmetrical heat transfer distributions is obtained.

It is seen from Figs. 4 and 5 that the plate motion has a little effect on the flow field and hence heat transfer distribution when the plate velocity is relatively small ($V_p/V_j = 0.1$). The shear-driven effects by the moving plate are not significant in this case and heat transfer distribution remains unchanged at the stagnation region. For a moderate

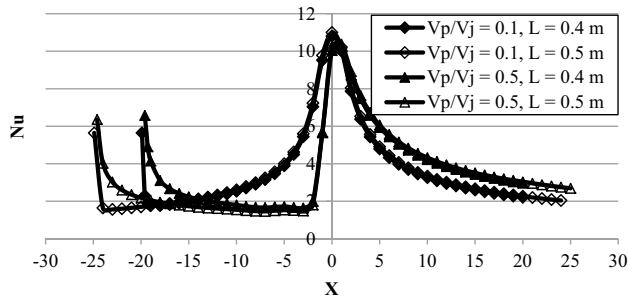


Fig. 6 Nusselt number distribution on the moving plate, $Re = 500$, $H/W = 5$, $L = 0.4$ and 0.5 m

plate velocity, $V_p/V_j = 0.5$, the left moving wall jet separates from the plate in a short distance from the impingement point due to the opposing shear generated by the right moving plate. It rises upwards slightly and continues to flow along the plate towards the left open boundary. As a result, a counterclockwise vortex is generated over the left part of the moving plate and heat transfer declines dramatically at this region. Heat transfer is somewhat enhanced at the right section of the moving plate due to the favorable plate motion. Finally, the shear-driven effects dominate over the entire plate surface and the enhanced heat transfer over the stagnation region is washed away at higher plate velocity ($V_p/V_j = 1$).

An overshoot is also observed in the Nusselt number distribution at the left open boundary where pressure outlet boundary condition is considered. The temperature of the shear-driven backflow at this boundary is the same as the nozzle exit temperature. Therefore, the plate surface temperature would be very close to the reference temperature giving rise to a higher heat transfer coefficient at that region. To investigate the effect of the location of this boundary on the Nusselt number distribution, the length of the plate was increased to 50 cm. Nusselt number distributions on the moving plate are illustrated in Fig. 6 for the

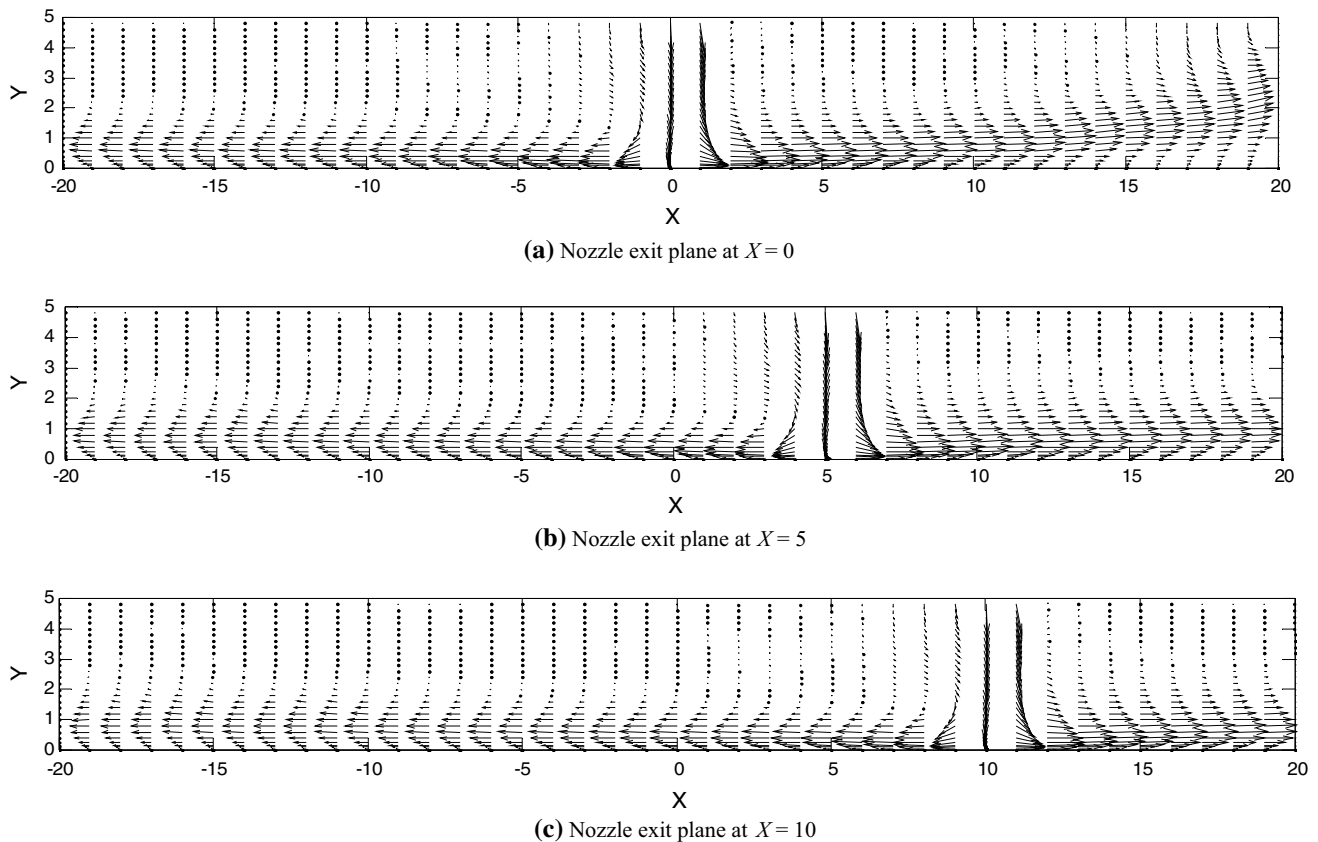


Fig. 7 Velocity vectors for the case of moving nozzle, $Re = 500$, $H/W = 5$ and $V_n/V_j = 0.1$

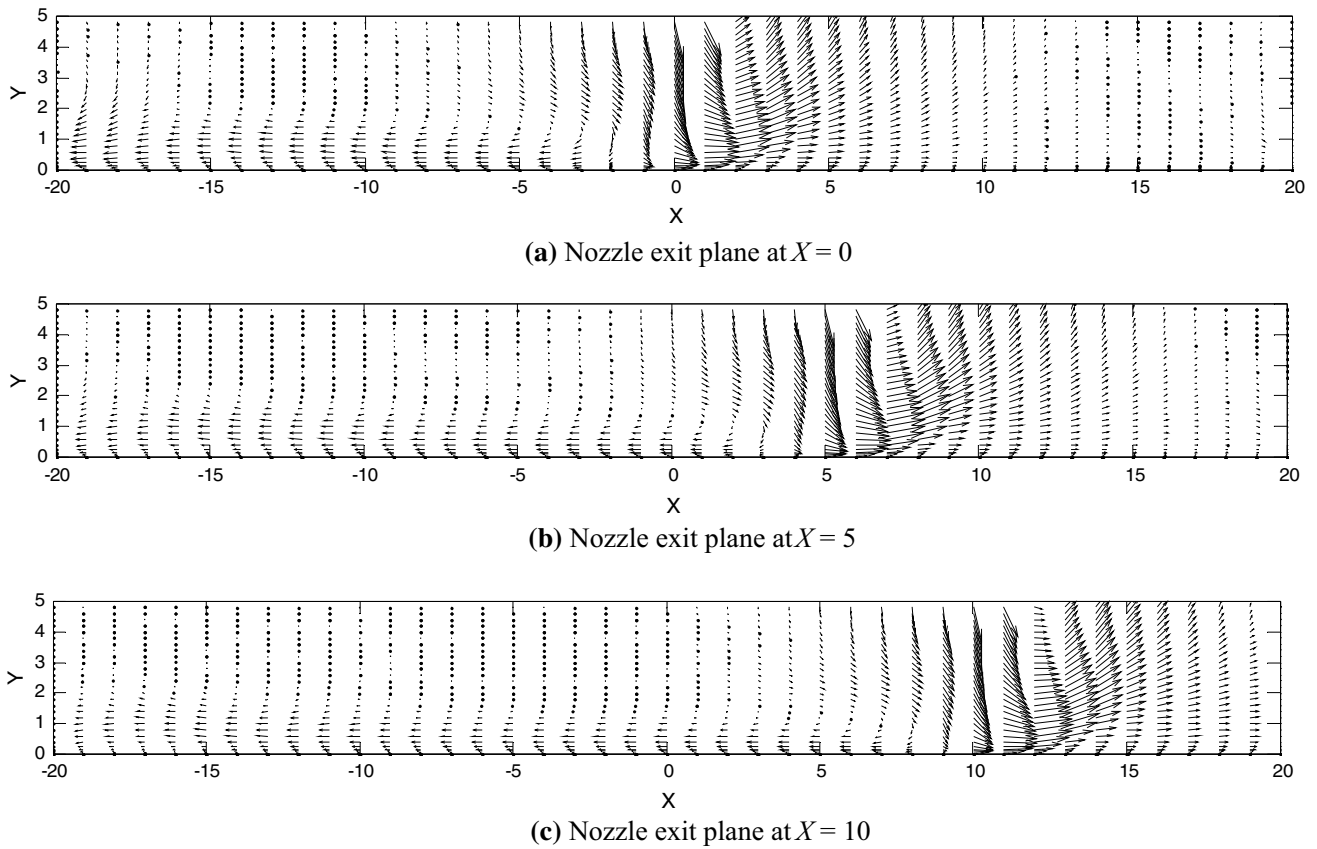


Fig. 8 Velocity vectors for the case of moving nozzle, $Re = 500$, $H/W = 5$ and $V_n/V_j = 0.4$

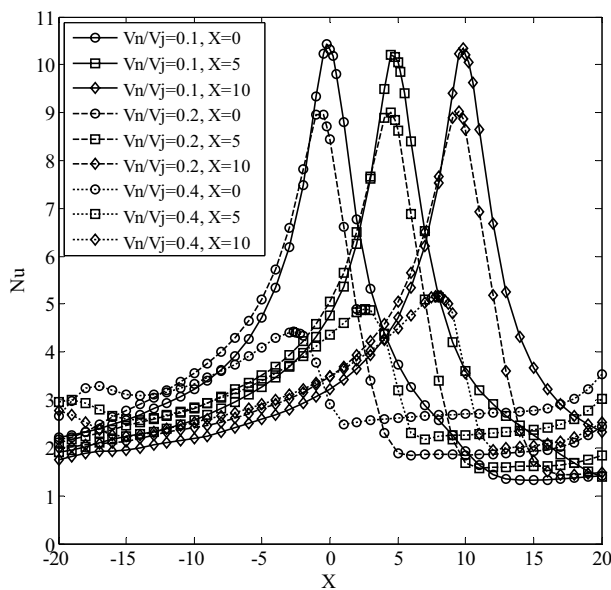


Fig. 9 Nusselt number distributions for moving nozzle, $Re = 500$, $H/W = 5$ and $V_n/V_j = 0.1, 0.2, \text{ and } 0.4$

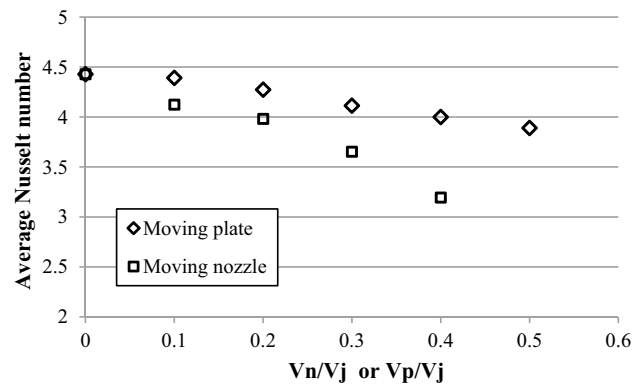


Fig. 10 Average Nusselt number for the moving plate and moving nozzle, $Re = 500$, $H/W = 5$

two examined plate lengths. This figure indicates that the location of the left open boundary has a very negligible effect on the Nusselt number distribution when the plate velocity is relatively small ($V_p/V_j = 0.1$). In addition, there is no significant change in the Nusselt number distribution

for moderate plate velocity except that the overshoot shifts to the end of the plate and, therefore, Nusselt number is slightly decreased on the left-hand side of the plate. This effect is only local and has little influence on the global flow and thermal fields except in the region close to the left open boundary.

Transient numerical analysis was then employed for the case of moving nozzle. The nozzle exit plane was assumed to be parallel to the impingement plate being initially at the position specified by $X = -15$. This exit plane was considered to move uniformly towards the right while the air jet was issuing into the domain. Vertical component of the air velocity was calculated from the Reynolds number definition. For air as the working fluid at 300 K and $Re = 500$, this velocity component was -0.764 m/s. Horizontal component of the air velocity at the exit plate was assumed to be the same as the nozzle velocity. The time step size for the numerical analysis was also evaluated using Eq. (1). Converged flow and thermal fields parameters were obtained at each time step and they were used as the initial conditions at the next time step sequentially. For $Re = 500$, $H/W = 5$ and $V_n/V_j = 0.1$ the velocity vectors are presented in Fig. 7 in which the nozzle exit plane is at various positions denoted by $X = 0, 5$, and 10 , respectively. Similar results for $V_n/V_j = 0.4$ are seen in Fig. 8 as representative results. In addition, corresponding Nusselt number distributions along with those of $V_n/V_j = 0.2$ and also stationary nozzle are shown in Fig. 9.

The flow fields represent that the right moving part of the flow is always stronger than the left moving part due to the moving nozzle effect. The right moving flow separates from the impingement plate in a short distance from the impingement region particularly for higher velocities of the moving nozzle. However, the left moving part of the flow continues to its motion towards the left open boundary along the impingement wall. Over the stagnation region, heat transfer distribution is very close to that of stationary nozzle when the velocity of the moving nozzle is small ($V_n/V_j = 0.1$). It continuously decreases all over the impingement plate as the velocity of the moving nozzle is increased. Meanwhile, the position of the overshoot in heat transfer distribution shifts towards left by increasing the velocity of the moving nozzle. Consistent with the flow field, heat transfer drops from the maximum value very smoothly in the left direction but the slope of the decline is very sharp in the opposite direction. Similar to the results of the moving plate, one small rise is also observed in the Nusselt number distribution at the left open boundary where pressure outlet boundary condition is considered which is a local and insignificant phenomenon. It is worth noting that by increasing the nozzle velocity even up to a moderate value ($V_n/V_j = 0.4$), the enhanced heat transfer at

the impinged region which is the main feature in jet impingent heat transfer, no longer persists at that region.

To compare the average cooling effect, which could be practically important, average Nusselt number over the central region of the impinged plate, $-15 < X < 15$ was evaluated for the various cases of the moving nozzle and plate. Figure 9 presents the calculated average Nusselt numbers. It is seen from this figure that the average Nusselt number decreases as the moving velocity of the plate or the nozzle is increased. However, it declines more rapidly for the case of moving nozzle so that the cooling effect would be very ineffectual even for a moderate nozzle velocity (Fig. 10).

5 Concluding remarks

For a laminar unconfined slot jet impinging on a flat plate, heat transfer distribution over the plate was specified for a range of relative velocity of the plate and the nozzle. Both the plate and the nozzle velocities had significant influence on the flow pattern and heat transfer distribution over the impinged plate. For the case of moving plate, the flow field was gradually dominated by the shear-driven flow due to the plate movement as the plate velocity was increased. For a moderate velocity of the nozzle, the co-moving part of the flow was separated from the impinged plate in a short distance while the other part flowed over the impinged plate consistently. Overall heat transfer was relatively small compared to the stationary case for both cases of the moving plate and the nozzle. Average Nusselt number dropped sharply in the case of moving nozzle.

References

1. Chattopadhyay H, Biswas G, Mitra NK (2000) Heat transfer from a moving surface due to impinging slot jets. *J Heat Transf* 124:433–440
2. Chattopadhyay H, Saha SK (2002) “Simulation of laminar slot jets impinging on a moving surface”. *J Heat Transf* 124:1049–1055
3. Miyazaki H, Silberman E (1972) Flow and heat transfer on a flat plate normal to a two-dimensional laminar jet issuing from a nozzle of finite height. *Int J Heat Mass Transf* 15:2097–2107
4. Rady M, Arquis E (2006) Heat transfer enhancement of multiple impinging slot jets with symmetric exhaust ports and confinement surface protrusions. *Appl Therm Eng* 26:1310–1319
5. Raju KS, Schlünder EU (1977) Heat transfer between an impinging jet and a continuously moving surface. *Wärme-und Stoffübertragung* 10(2):131–136
6. Senter J, Sollic C (2007) Flow field analysis of a turbulent slot jet impinging on a moving flat surface. *Int J Heat Fluid Flow* 28:708–719
7. Sharif MA, Banerjee A (2009) Numerical analysis of heat transfer due to confined slot-jet impingement on a moving plat. *Appl Therm Eng* 29:532–540

8. Yang YT, Hao TP (1999) Numerical studies of three turbulent slot jets with and without moving surface. *Acta Mech* 136:17–27
9. Zumbrunnen DA, Incropera FP, Viskanta R (1992) A laminar boundary layer model of heat transfer due to a non uniform planar jet impinging on a moving plate. *Wärme-und Stoffübertragung* 27(5):311–319